

iScience, Volume 24

Supplemental information

**Water-dispersible Ti₃C₂T_z MXene
nanosheets by molten salt etching**

Kailash Arole, Jackson W. Blivin, Sanjit Saha, Dustin E. Holta, Xiaofei Zhao, Anubhav Sarmah, Huaixuan Cao, Miladin Radovic, Jodie L. Lutkenhaus, and Micah J. Green

Water-dispersible $Ti_3C_2T_z$ MXene Nanosheets by Molten Salt Etching

Kailash Arole¹, Jackson W. Bilvin², Sanjit Saha², Dustin E. Holta¹, Xiaofei Zhao², Anubhav Sarmah², Huaixuan Cao², Miladin Radovic¹, Jodie L. Lutkenhaus^{1,2}, Micah J. Green^{1,2*}

¹Department of Materials Science and Engineering, Texas A&M University, College Station, TX 77843, USA

²Artie McFerrin Department of Chemical Engineering, Texas A&M University, College Station, TX 77843, USA

*Corresponding author: micah.green@tamu.edu

Supplementary Information

Fig. S1. $Ti_3C_2T_z$ processing schematic

Fig. S2. EDS mapping of $Ti_3C_2T_z$ clay a) before KOH washing b) after KOH washing

Table S1. EDS data which shows the elemental composition of the $Ti_3C_2T_z$ clay before and after KOH washing

Fig. S3 Stable aqueous dispersion of $Ti_3C_2T_z$ nanosheets with negative ζ potential

Fig. S4. Two-Stage centrifugation method schematic

Fig. S5. Additional SEM images of $Ti_3C_2T_z$ nanosheets

Fig. S6. AFM image of $Ti_3C_2T_z$ nanosheet and corresponding height profile

Fig. S7. UV–Vis absorption spectra of $Ti_3C_2T_z$ dispersion

Data S1. $Ti_3C_2T_z$ MXene formation mechanism

Fig. S8. RF response heating profile and Thermal Images of RF response of $Ti_3C_2T_z$

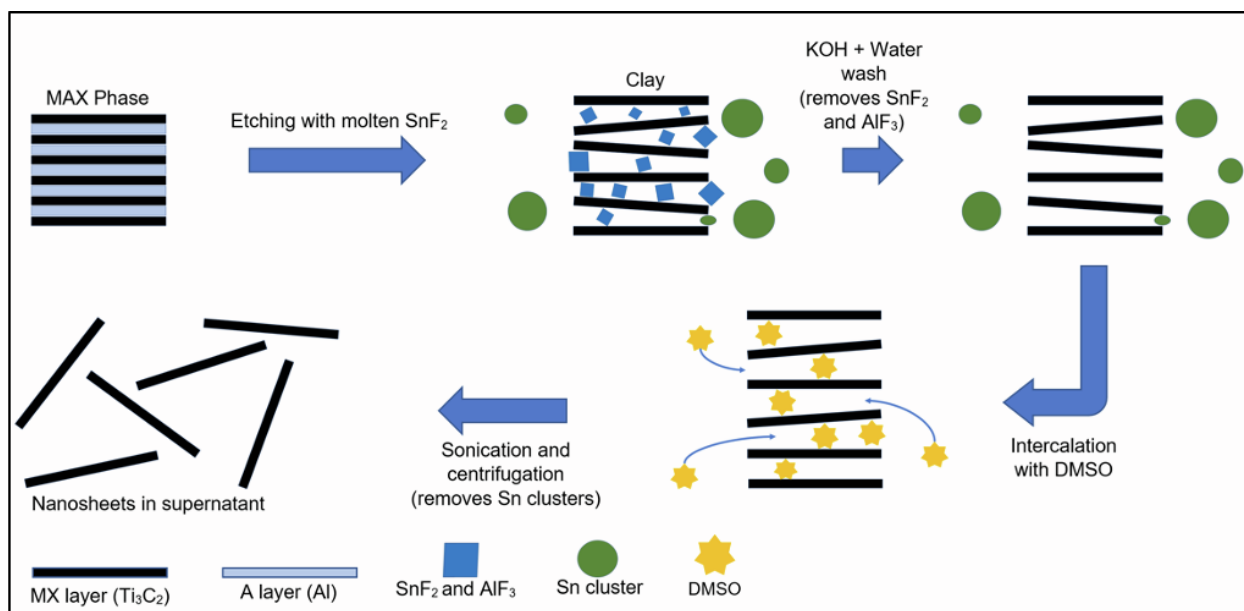


Fig. S1. $Ti_3C_2T_x$ processing schematic, which clearly shows every step need to be followed to get $Ti_3C_2T_x$ dispersion. Related to STAR Methods.

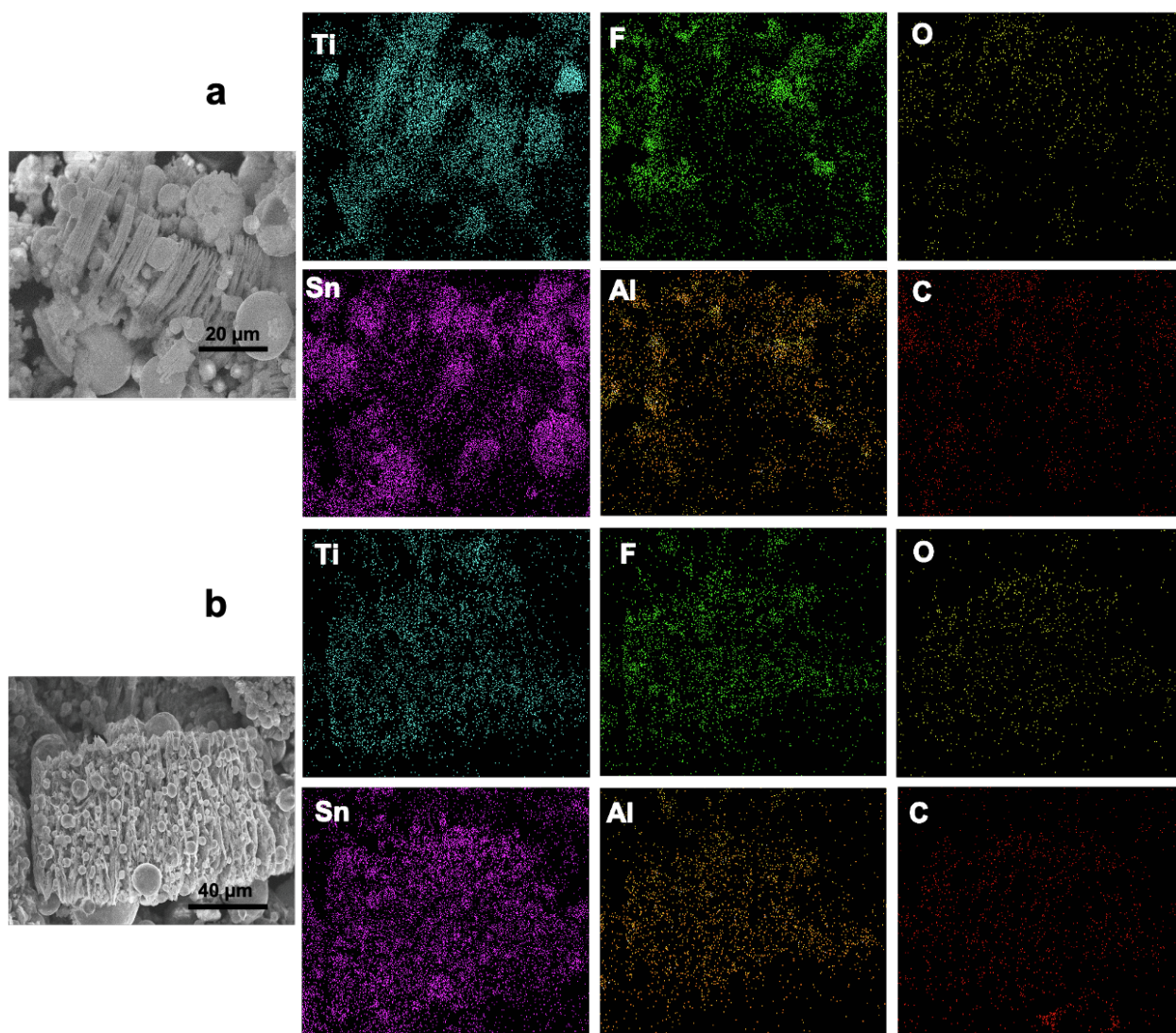


Fig. S2. EDS mapping of $Ti_3C_2T_x$ clay a) before KOH washing b) after KOH washing. Related to figure 2.

Table S1. EDS data which shows the elemental composition of the $Ti_3C_2T_z$ clay before and after KOH washing corresponding to Fig. S2. The highlighted red shows the reduced percentage of aluminum compared to MAX phases which indicated the successful etching. Related to figure 2.

MXene	Before KOH wash	After KOH wash
Element	% Weight	% Weight
C	8.25	9.24
O	6.64	11.00
F	37.43	33.43
Al	2.90	2.86
Ti	11.97	8.02
Sn	31.97	35.19

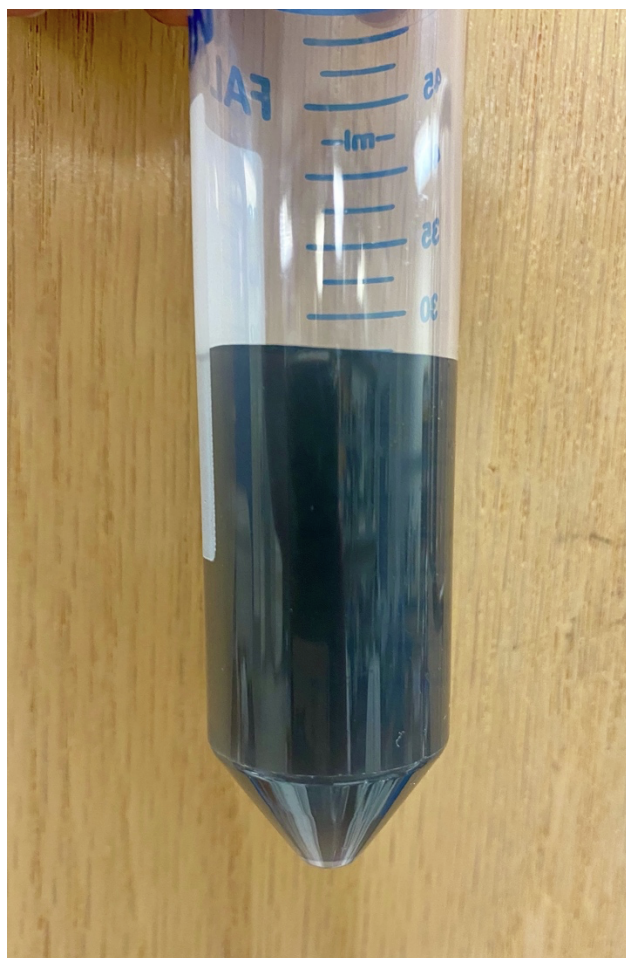


Fig. S3. Stable aqueous dispersion of $\text{Ti}_3\text{C}_2\text{T}_z$ nanosheets with negative ζ potential. Related to figure 3.

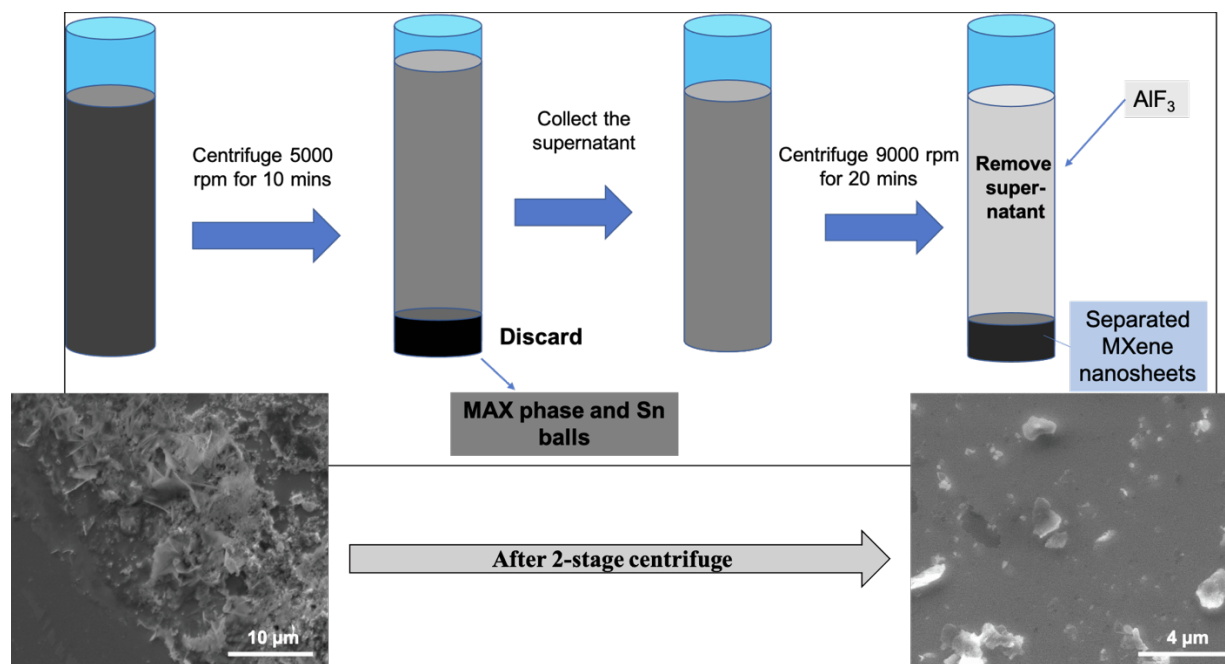


Fig. S4. Two-Stage centrifugation method used for the separation of $Ti_3C_2T_z$ from the Sn Spheres. This method helped to get rid of heavy MAX phase particles and other small unwanted particles from the supernatant. The original dispersion (SEM, left) has considerable Ti_3AlC_2 MAX phase, Sn spheres, etc. present, whereas the final product (SEM, right) is composed of Ti_3C_2 nanosheets. Related to STAR Method.

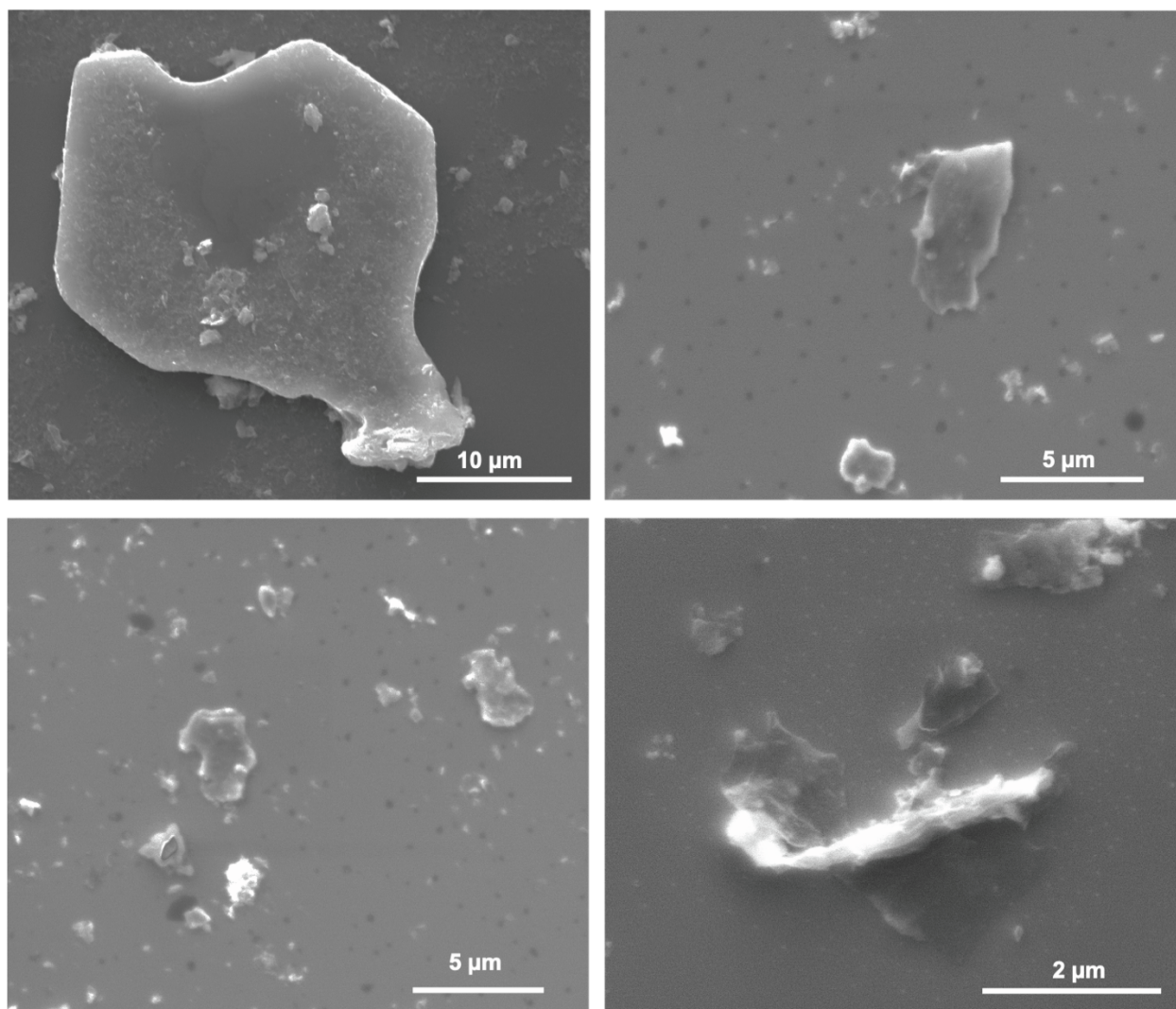


Fig. S5. Additional SEM images of $\text{Ti}_3\text{C}_2\text{T}_z$ nanosheets, which confirms the formation of single layer MXene nanosheets. Related to figure 2.

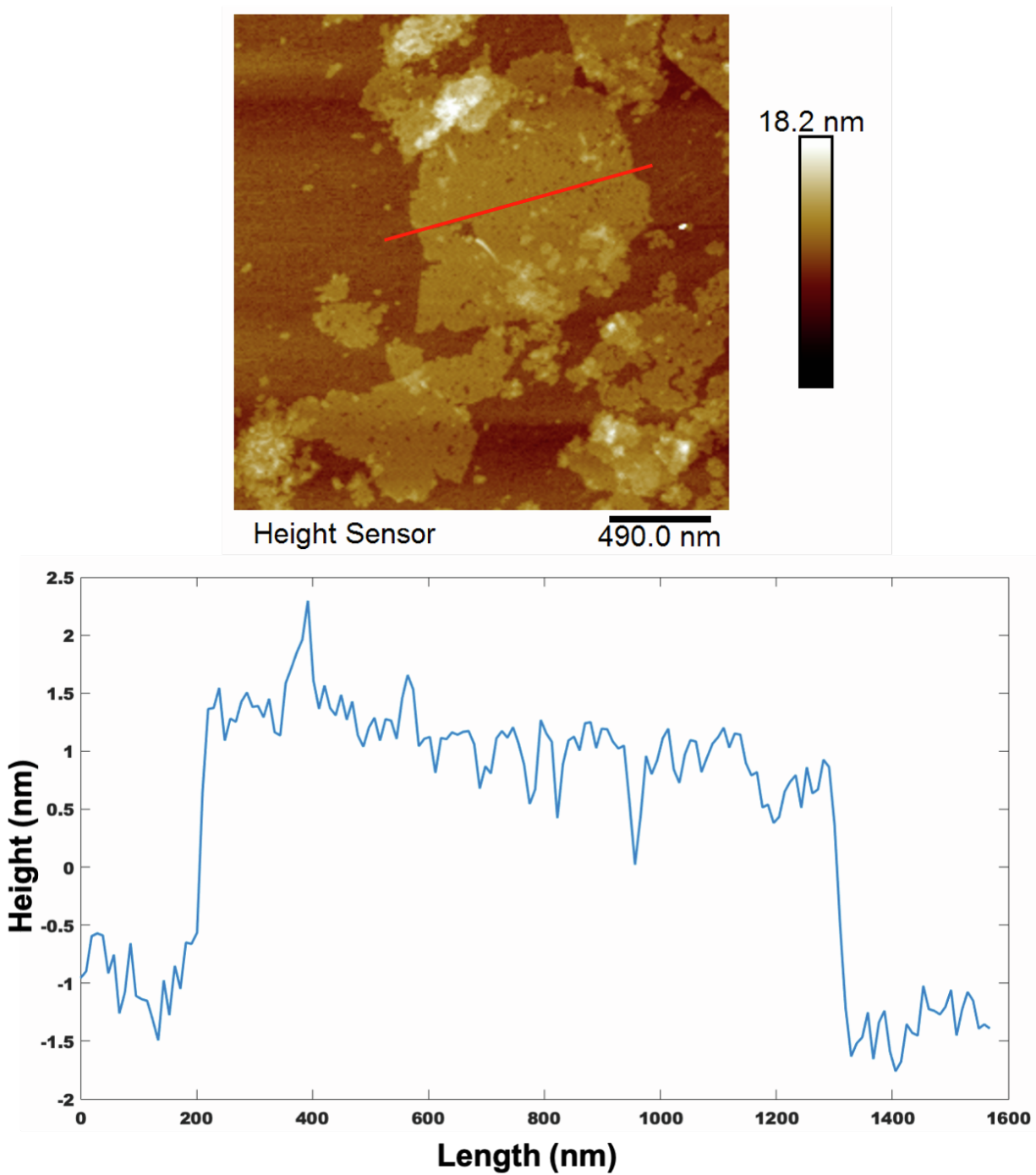


Fig. S6. AFM image of $\text{Ti}_3\text{C}_2\text{T}_z$ nanosheet and corresponding height profile. $\text{Ti}_3\text{C}_2\text{T}_z$ dispersion was again diluted with water and drop-cast on freshly cleaved mica substrate. The concentration of sample used for AFM was 0.006 mg/ml. Related to figure 6.

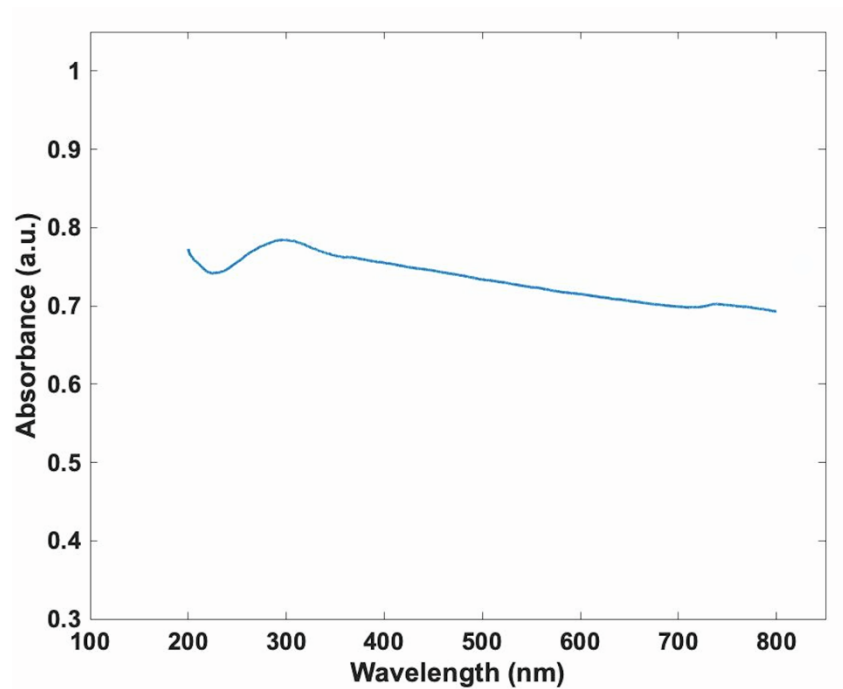
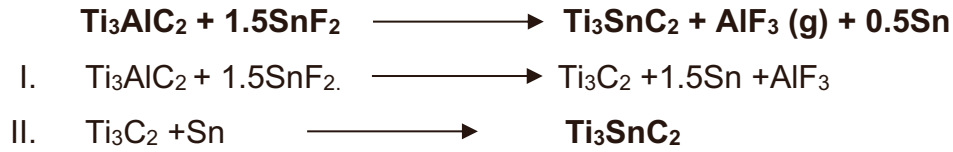


Fig. S7. UV–Vis absorption spectra of $\text{Ti}_3\text{C}_2\text{T}_z$ dispersion (0.4 mg/ml), which clearly resembles with the acid etched $\text{Ti}_3\text{C}_2\text{T}_z$ dispersion. Related to STAR Methods.

Data S1. $\text{Ti}_3\text{C}_2\text{T}_z$ MXene Formation Mechanism. Related to figure 1.

The formation of F-terminated $\text{Ti}_3\text{C}_2\text{T}_z$ is a two-step process as reported by Mian *et al.* (Li *et al.*, 2019), which we recapitulate here. **Step 1** involves the replacement of Al in Ti_3AlC_2 by Sn that results in the formation Ti_3SnC_2 , which is an intermediate product in the formation of $\text{Ti}_3\text{C}_2\text{T}_z$ along with AlF_3 as a byproduct is generated. Also, as the reaction proceeds, Sn^{2+} ions form, which will intercalate into A site after removal of Al from Ti_3AlC_2 .

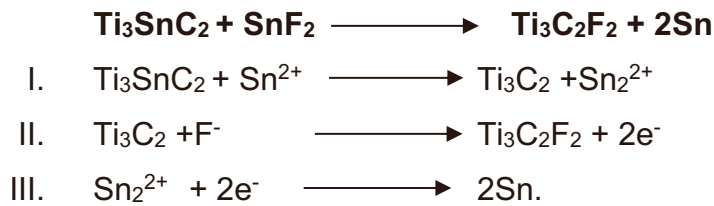
Step 1



The formation of F-terminated $\text{Ti}_3\text{C}_2\text{T}_z$ depends on the ratio of the Al-MAX phase to SnF_2 . The ratio of the Al-MAX phase to SnF_2 used in this study is 1:6. The exact mechanism behind the formation of $\text{Ti}_3\text{C}_2\text{T}_z$ was not clearly stated in the study by Mian *et al.* (Li *et al.*, 2019).

The formation of F-terminated $\text{Ti}_3\text{C}_2\text{T}_z$ from an intermediate product Ti_3SnC_2 is represented in **Step 2**, which is further subdivided into three steps. Previous research indicated that the redox reaction between Sn and Sn^{2+} results in the dissolution of Sn into a molten SnF_2 . The weakly bonded Sn atoms in Ti_3SnC_2 were easily removed from the A-site and dissolved into a molten salt SnF_2 . The F^- anions spontaneously intercalated into the A-site plane of Ti_3C_2 and bonded with specific site of Ti_3C_2 to form more stable F-terminated $\text{Ti}_3\text{C}_2\text{T}_z$.

Step 2



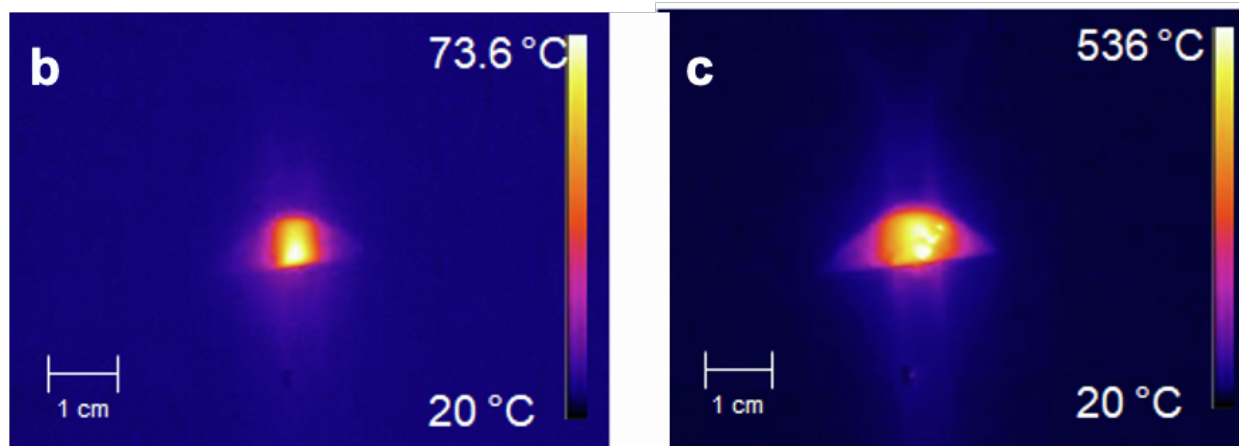
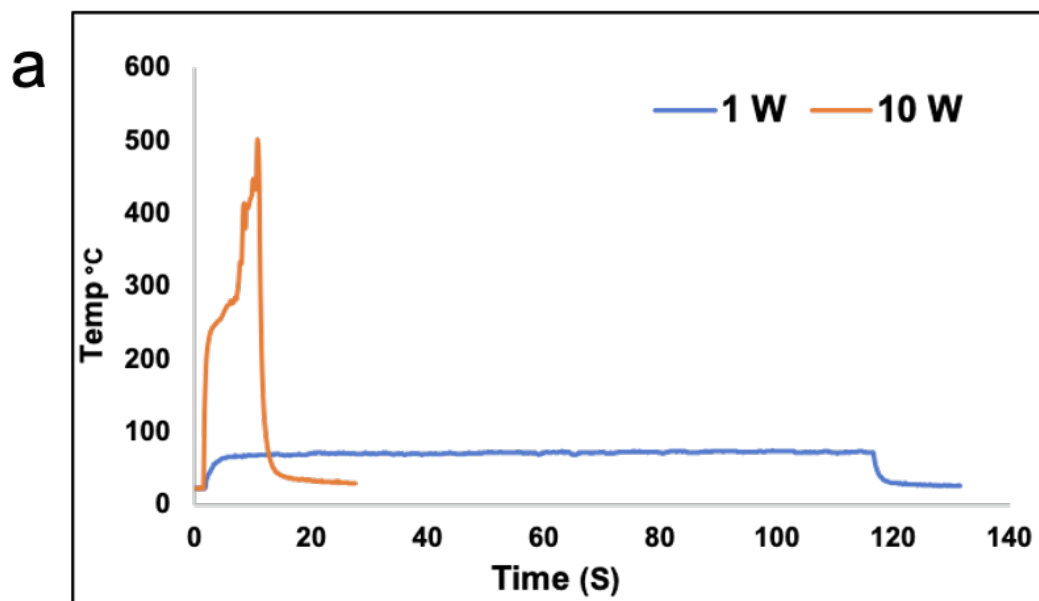


Fig. S8. a) Radio Frequency (RF) response of $\text{Ti}_3\text{C}_2\text{T}_z$ at 1 W (135 MHz) and 10 W (135 MHz) power; b) Thermal Images of RF response of $\text{Ti}_3\text{C}_2\text{T}_z$ at 1 W (135 MHz) and; c) 10 W (135 MHz) power. Related to STAR Methods.

References:

LI, M., LU, J., LUO, K., LI, Y., CHANG, K., CHEN, K., ZHOU, J., ROSEN, J., HULTMAN, L., EKLUND, P., PERSSON, P. O. Å., DU, S., CHAI, Z., HUANG, Z. & HUANG, Q. 2019. Element Replacement Approach by Reaction with Lewis Acidic Molten Salts to Synthesize Nanolaminated MAX Phases and MXenes. *Journal of the American Chemical Society*, 141, 4730-4737.